A liver HIF-2α/IRS2 pathway sensitizes hepatic insulin signaling and is modulated by VEGF inhibition

Kevin Wei[#1], **Stephanie M. Piecewicz**[#1], **Lisa M. McGinnis**[#1], **Cullen M. Taniguchi**[2], **Stanley J. Wiegand**[3], **Keith Anderson**[3], **Carol W-M. Chan**[1], **Kimberly X. Mulligan**[4], **David Kuo**[1], **Jenny Yuan**[1], **Mario Vallon**[1], **Lori Morton**[3], **Etienne Lefai**[5], **M. Celeste Simon**[6], **Jacquelyn J. Maher**[7], **Gilles Mithieux**[8], **Fabienne Rajas**[8], **Justin Annes**[9], **Owen P. McGuinness**[4], **Gavin Thurston**[3], **Amato J. Giaccia**[2], and **Calvin J. Kuo**[1]

[1]Division of Hematology, Stanford University School of Medicine, Stanford, California 94305, USA

[2]Division of Radiation Oncology Stanford University School of Medicine, Stanford, California 94305, USA

[3]Regeneron Pharmaceuticals, Incorporated, Tarrytown, New York, 10591, USA

[4]Department of Molecular Physiology and Biophysics, Vanderbilt University School of Medicine, Nashville TN 37232, USA

[5]INSERM U 1060, INRA 1235, Universite de Lyon, Faculté de Médecine Lyon Sud - BP12, 69921 OULLINS Cedex, France

[6]Abramson Family Cancer Research Institute, Howard Hughes Medical Institute, University of Pennsylvania School of Medicine, Philadelphia, Pennsylvania, 19104, USA

[7]UCSF Liver Center, San Francisco General Hospital, 1001 Potrero Ave. Building 40, Room 4102, San Francisco, CA 94110

[8]Inserm U855/Université Lyon, Faculté Lyon Est Laennec, 7 rue Guillaume Paradin, 69372 Lyon cedex 08, France

[9]Division of Endocrinology and Metabolism, Stanford University School of Medicine, Stanford, California 94305, USA

[#] These authors contributed equally to this work.

Abstract

Insulin initiates diverse hepatic metabolic responses, including gluconeogenic suppression and induction of glycogen synthesis and lipogenesis[1,2]. The liver possesses a rich sinusoidal capillary

network with increased hypoxia and decreased gluconeogenesis in the perivenous zone[3]. Here, diverse vascular endothelial growth factor (VEGF) inhibitors improved glucose tolerance in normal or diabetic *db/db* mice, potentiating hepatic insulin signaling, decreasing gluconeogenic gene expression, increasing glycogen storage and suppressing hepatic glucose production (HGP). VEGF inhibition induced hepatic hypoxia via sinusoidal vascular regression and sensitized liver insulin signaling through hypoxia inducible factor-2α (HIF-2α) stabilization. Notably, liver-specific constitutive activation of HIF-2α, but not HIF-1α, was sufficient to augment hepatic insulin signaling via direct and indirect induction of insulin receptor substrate 2 (IRS2), an essential insulin receptor adaptor protein[4–6]. Further, liver IRS2 was both necessary and sufficient to mediate HIF-2α and VEGF inhibition effects on glucose tolerance and hepatic insulin signaling. These results demonstrate an unsuspected intersection between HIF-2α–mediated hypoxic signaling and hepatic insulin action via IRS2 induction, which can be co-opted by VEGF inhibitors to modulate glucose metabolism. These studies also indicate distinct roles in hepatic metabolism for HIF-1α, which promotes glycolysis[7–9], versus HIF-2α, which suppresses gluconeogenesis, and suggest novel treatment approaches for type 2 diabetes mellitus.

The liver regulates systemic energy reserves by controlling carbohydrate and lipid metabolism in response to dietary and systemic cues. Hepatic insulin stimulation recruits insulin receptor substrate (IRS) proteins to the insulin receptor, with activation of AKT, GSK3β and mTOR, coordinately suppressing hepatic gluconeogenesis and inducing glycogen synthesis and lipogenesis[1,2]. The liver perivenous zone experiences relative hypoxia accompanied by suppression of gluconeogenesis[3]. During normoxia, prolyl hydroxylase domain–containing enzymes (PHD1–3) and factor inhibiting HIF (FIH) hydroxylate members of the HIF transcription factor family (HIF1–3), resulting in von Hippel-Lindau (VHL)-dependent proteosomal degradation; hypoxic inhibition of this hydroxylation stabilizes HIFs and induces HIF transcriptional targets[10].

The VEGF family contains VEGF-A-D and PlGF, each with distinct affinities for VEGF receptors 1–3 (VEGFR1–3) and neuropilins. VEGFR1/Flt1 is a high-affinity receptor for VEGF-A, -B and PlGF versus VEGFR2/Flk1, which is a low-affinity receptor for VEGF-A, -C and –D[11,12]. VEGF inhibitor treatment decreases fasting blood glucose levels and improves glucose tolerance in mice and humans through unclear mechanisms[13,14], and specific VEGF-B inhibition improves glucose tolerance through enhanced peripheral glucose uptake[15]. Here, we utilized single intravenous injection of adenoviruses encoding the soluble extracellular ligand-binding domains of VEGFR1/Flt1 (Ad sFlt1) or VEGFR2/Flk1 fused to an antibody Fc fragment (Ad sFlk1) to achieve hepatic secretion of Flt1 or Flk1 ectodomains into the circulation; both ectodomains elicit potent and durable VEGF-A neutralization *in vivo*[16,17]. Ad sFlt1-mediated VEGF inhibition improved the response to i. p. glucose injection in both glucose tolerance tests (GTT) and insulin tolerance tests (ITT) in either C57Bl/6 (Fig. 1a) or diabetic *db/db* mice (Fig. 1b) compared to control treatment as confirmed by AUC analysis (Supplementary Fig. 1a–d). Similar results were obtained with Ad sFlk1 (Fig. 1b and Supplementary Fig. 1c,d). Recombinant aflibercept/VEGF Trap, encoding a VEGFR1/VEGFR2 ectodomain fusion that binds VEGF-A, -B and PlGF[18,19], also improved glucose tolerance versus control treatment in C57Bl/6 or *db/db* mice (Fig. 1c, d and Supplementary Fig. 1e,f), as did both the anti-VEGF-A monoclonal antibody (mAb)

B20.4.1.1[20], and the anti-VEGFR2 monoclonal antibody DC101[21] (Supplementary Fig. 1g,h), neither of which interfere with VEGF-B signaling.

VEGF inhibitors decreased fasting or fed glucose levels (Supplementary Fig. 2a–e) and aflibercept did not increase plasma insulin or decrease glucagon (Supplementary Fig. 2f,g). In a hyperinsulinemic euglycemic clamp study, two-week aflibercept treated *db/db* mice exhibited higher insulin sensitivity, enhanced insulin-induced suppression of hepatic glucose production (HGP) (Fig. 1e and Supplementary Fig. 3) and substantially improved hyperinsulinemia (Fig. 1f) compared to control hFc-treated *db/db* mice. This occurred without altering insulin-stimulated whole-body glucose disposal, peripheral tissue-specific glucose uptake, or hepatic CREB or AMPK signaling (Supplementary Fig. 4a,b).

The insulin-potentiating effects of VEGF inhibition on HGP prompted evaluation of insulin receptor (IR) signaling in liver. Both aflibercept and Ad sFlt1 treatment increased phosphorylation of AKT (p-AKT) and GSK3β (p-GSK3β), augmented expression of IRS2, but not IRS1 or IR itself (Fig. 1g, h), and suppressed phosphoenolpyruvate kinase (*Pepck*) and glucose-6-phosphatase catalytic subunit (*G6pc*) versus controls (Fig. 1i,j). Similar effects were also observed with Ad sFlk1 treatment (Fig. 1i and Supplementary Fig. 4c,d). Both sFlt1 and sFlk1 repressed liver G6PC and elevated glycogen in fasted liver compared to Fc-treated mice (Supplementary Fig. 4e). Together, this data indicated that VEGF inhibition suppresses HGP through hepatic insulin signaling sensitization.

VEGF inhibition induces capillary regression in both normal adult organs and solid tumors, although effects in liver have not been described[13,22,23]. Ad sFlt1, Ad sFlk1 and recombinant aflibercept induced marked and reversible regression of CD31^{+} hepatic sinusoids compared to controls (Fig. 2a,b and Supplementary Fig. 5a,b), as did DC101 and B20.4.1.1 (Supplementary Fig. 5c,d). A sensitive FACS-based hypoxyprobe method detected a clear hypoxic shift in liver upon *in vivo* VEGF antagonism (Fig. 2c) versus Fc-treated animals. Ad sFlt1 and aflibercept also decreased functional perfusion in mouse liver upon intravascular biotin infusion (Fig. 2d). Further, microarray analysis of aflibercept-treated mouse liver revealed upregulation of several hypoxia-inducible genes, including *Cited2*, *Loxl2*, and *Pfk1* (Supplementary Fig. 6a), while HIF-2α, but not HIF-1α protein was stabilized in Ad sFlt1-treated mouse liver (Fig. 2e). Notably, Ad sFlt1 improved glucose tolerance in unexcised *Hif2α*^*flox/flox*^ mice, but this effect was significantly blunted upon liver-specific *Hif-2α* deletion (*Hif-2α* LKO) in *Hif2α*^*flox/flox*^*;albumin-Cre* mice[9] (Fig. 2f and Supplementary Fig. 7a). Similarly, Ad sFlt1 induction of hepatic IRS2, p-AKT or p-GSK3β and *G6pc* suppression was blunted in *Hif-2α* LKO mice (Fig. 2g,h), indicating that VEGF inhibition requires liver Hif2α to sensitize liver insulin signaling. Additionally, adenoviral shRNA knockdown of liver Hif2α also reversed sFlt1 effects on glucose tolerance and insulin signaling (Supplementary Fig. 7b–e).

We next examined whether hepatic HIF-2α activation was sufficient to augment liver insulin receptor signaling. Adenoviral hepatic expression of a constitutively active allele of Hif2α mutated at inhibitory hydroxylation sites Pro531 and Asn847 (Ad Hif2αPN) or lacking the inhibitory oxygen-dependent degradation domain (ODD) (Ad Hif2α ODD) significantly improved glucose tolerance, blood glucose and insulin tolerance under fed or

fasted conditions compared to Ad Fc controls; a Hif1α ODD mutant had comparatively less activity (Fig. 3a and Supplementary Fig. 8a–f). Similarly, Ad Hif2αPN or Ad Hif2α ODD elevated hepatic IRS2 protein, p-AKT, p-GSK3β and p-FOXO1 under fasted or fed conditions while Hif1α ODD was comparatively less active (Fig. 3b,c and Supplementary Fig. 8g). In parallel, HIF-2α constitutive activation repressed *G6pc* and *Pepck* more strongly than did HIF-1α (Fig. 3d and Supplementary Fig. 8h). In primary mouse hepatocytes, HIF-2α but not HIF-1α activation markedly elevated IRS2 levels and potently synergized with insulin to elevate AKT phosphorylation compared to control, indicating a cell-autonomous mechanism (Fig. 3e).

The functional relevance of IRS2 to HIF-2α regulation of hepatic insulin signaling was explored both *in vitro* and *in vivo*. In primary hepatocytes, the synergistic activation of AKT phosphorylation by Ad Hif2αPN and insulin was attenuated by *Irs2* knockdown (Ad shRNA IRS2) (Fig. 3f). Further, in *db/db* mice, the ability of Ad Hif2αPN to improve glucose tolerance, increase liver AKT phosphorylation and repress *G6pc* were attenuated by concomitant *Irs2* knockdown (Fig. 3g,h and Supplementary Fig. 8i). Hepatic *Irs2* overexpression via Ad IRS2 markedly improved glucose tolerance in *db/db* mice versus Ad Fc in agreement with previous results[24] and phenocopied Ad Hif2αPN or VEGF inhibition (Fig. 3i and Supplementary Fig. 8j), consistent with liver IRS2 induction being sufficient to mediate Ad Hif2αPN or VEGF inhibition effects on glucose tolerance. Similarly, Ad sFlt1 improvement of glucose tolerance was also attenuated by liver *Irs2* shRNA knockdown (Fig. 3j).

HIF-2α induced liver *Irs2* mRNA both in vivo and in primary hepatocytes (Fig. 4a,b), suggesting direct transcriptional regulation. Canonical hypoxia-response elements (HREs) are present at −900 and −123 in the mouse and human IRS promoter regions (Fig. 4c). The proximal −123 but not the distal −900 HRE was required for HIF-2α transactivation of an IRS2-luciferase reporter construct in insulin-starved H2 hepatoma cells; notably, HIF-1α was ineffective (Fig. 4c) and both HIF-1α and HIF-2α potently activated 5xHRE luciferase constructs (data not shown). Additionally, microarray of aflibercept-treated mouse liver revealed down-regulation of numerous SREBP-1c target genes (Supplementary Fig. 6b). In addition to well-described lipogenic functions and induction by feeding or insulin[1], SREBP-1c represses *Irs2* in fed or fasted mice by competitively inhibiting FOXO binding to *Irs2* promoter insulin responsive elements[25]. Further, liver *Srepb1c* and *Irs2* expression are inversely correlated in multiple settings[25,26], suggesting possible HIF-2α induction of IRS2 via *Srebp1c* repression. Constitutive HIF-2α activation potently abrogated both insulin-stimulated *Srebp-1c* expression in primary hepatocytes (Fig. 4d) and *Srebp-1c* expression in fed mice (Fig. 4e). However, HIF-1α activation also lowered *Srebp-1c* mRNA levels (Fig. 4e) without affecting glucose tolerance or inducing IRS2 (Fig. 3, Supplementary Fig. 8a–g), suggesting that *Srebp1c* repression was not itself sufficient for HIF-2α induction of IRS2. Forced adenoviral overexpression of a cleaved active form of SREBP-1c (Ad nSrebp1c)[27] reversed Ad Hif2αPN stimulation of IRS2 both in insulin-starved primary hepatocytes (Fig. 4f) and in vivo under re-fed conditions (Fig. 4g). Thus, HIF-2α suppression of the *Irs2* repressor *Srebp1c*, while not itself sufficient, facilitates HIF-2α–*Irs2* direct trans-activation (Fig. 4h).

These studies reveal a previously unsuspected cross-talk between the liver hypoxia and insulin signaling pathways whereby HIF-2α strongly augments insulin-dependent AKT activation and gluconeogenic suppression (Fig. 4h). Here, complementary *in vitro* and *in vivo* studies demonstrate that HIF-2α positively regulates hepatic insulin signaling by up-regulating IRS2. This IRS2 induction is specific to HIF-2α and not HIF-1α, paralleling studies where the former and not the latter exerts dominant roles in regulation of liver lipogenesis[32], of hepatic *Epo*[9,28] and of other loci such as *Oct4*, *cyclin D1* and *DMT1*[29–31]. In knockdown and overexpression studies, liver IRS2 is both necessary and sufficient for HIF-2α-mediated improvement of glucose tolerance and hepatic insulin signaling. The improved glucose tolerance upon liver IRS2 overexpression agrees strongly with prior studies where increased hepatic IRS2 expression is fully sufficient to potently ameliorate diabetes in *db/db* mice and activate fasted liver insulin signaling[24].

Although we have established a clear functional role for IRS2, we cannot fully exclude parallel IRS2-independent pathways. Possibilities for IRS2-independent HIF effects include insulin-independent, direct association of PGC-1α, HNF4 and/or C/EBPα with *Pepck* and *G6pc* promoter elements[32,33]. Alternatively, EPO has been reported to either improve peripheral glucose uptake[34] or inhibit gluconeogenesis by modulation of inflammation[35], although EPO does not induce liver IRS2 (S. P. and C. J. K., unpublished data). Our demonstration that the HIF-2α/ IRS2 axis couples hypoxia sensing to gluconeogenic repression via potentiation of hepatic insulin signaling complements observations of hypoxic regulation of IRS2 and invasion in breast cancer cells[36]. Notably, upon hepatic *Vhl* deletion stabilizing both HIF-2α and HIF-1α, a *Srebp1c* gene signature is induced by superimposed deletion of *Hif2*α but not *Hif1*α, suggesting the possibility of HIF-2α-specific *Srebp1c* repression[32]. HIF-2α induced IRS2 but decreased IRS1, suggestive of potential reciprocal regulation; however, liver IRS1 down-regulation typically impairs rather than improves glucose tolerance[4,5].

The beneficial effects of HIF-2α on animal models of insulin resistance suggest the potential therapeutic utility of prolyl hydroxylase inhibitors that block VHL-dependent HIF degradation for type 2 diabetes mellitus therapy. This could occur via isoform-specific PHD3 pharmacologic inhibition (see accompanying paper by Taniguchi et al.) that could circumvent the hepatic lipid accumulation associated with conventional liver HIF-2α activation.[32,37] A second strategy for pharmacologic manipulation of the hepatic HIF-2α/ IRS2 axis is represented by VEGF inhibition, which decreases pancreatic islet microvessel density[13] with specific VEGF-B antagonism enhancing peripheral glucose uptake[15]. However, we describe that VEGF inhibitors such as aflibercept, which binds VEGF-A, -B and PlGF[18], can exert primary action on liver via insulin sensitization rather than on skeletal muscle. Such alternative mechanisms are further supported by the ability of non-VEGF-B VEGF inhibitors such as sFlk1, B20.4.1.1 and DC101 to modulate glucose tolerance and/or hepatic insulin signaling. Conceivably, VEGF-A and VEGF-B could coordinately regulate glucose metabolism via hepatic insulin signaling and peripheral glucose uptake, respectively[15], with additional mechanisms certainly possible. Since HIF-2α and HIF-1α exhibit similar hypoxic stabilization profiles[38], the specific VEGF inhibitor stabilization of HIF-2α versus HIF-1α could occur via selective PHD3 inhibition (see accompanying

manuscript by Taniguchi et al.) or alternative non-hypoxic pathways[17], and underlie observations of improved glucose control in diabetic VEGF inhibitor-treated patients[14]. It is further interesting to contemplate the potential contribution of decreased plasma glucose to anti-tumor effects of VEGF inhibition[39].

Overall, our data indicate distinct roles in energy metabolism for hepatic HIF-2α, which sensitizes liver insulin signaling and suppresses gluconeogenesis, versus hepatic HIF-1α, which promotes glycolysis[7–9]. In vivo, physiologic perivenous liver hypoxia[3] could trigger the HIF-2α/IRS2 axis, preferentially enhance insulin signaling and suppress perivenous *Pepck* and *G6pc*, explaining the enrichment of gluconeogenesis in the periportal zone[3]. Finally, the mechanistic interplay in liver between the hypoxia/HIF-2α and insulin receptor signaling pathways, as demonstrated here, has potentially broad implications for the study of metabolism and therapeutic approaches to type 2 diabetes mellitus.

Online Methods

Animals

All mice were males and on a 12-h light/dark cycle in a pathogen-free animal facility and unless otherwise specified were C57Bl/6J (JAX). The generation of Hif2α conditional alleles and albumin-Cre transgenic mice have been previously described[40,41]. Hepatocyte-specific deletion of Hif2α was achieved through generating mice that were homozygous for the Hif2α 2-lox alleles and expressed the albumin-Cre transgene. Littermates not carrying the albumin-Cre transgene were used as control animals. Mutant mice were generated in a mixed genetic background (BALB/c, 129Sv/J, and C57BL/6). 8–10 week-old Lepr *db/db* and Lepr *db/+* mice were purchased from Jackson Laboratory. 8–10 week-old C57BL/6 mice were purchased from Taconic. Mice were injected with adenoviruses through the tail vein at between 1×10^8 to 5×10^8 plaque-forming units in 0.1 mL PBS. (Ad sFlt1, Ad sFlk1, Ad Fc 1×10^9 pfu; Ad HIF2αPN, Ad HIF2 ODD, Ad HIF1 ODD, Ad IRS2, Ad Fc 3×10^8 and 1.5×10^8; Ad shRNA IRS2, Ad shRNA luciferase 5×10^8 and 6×10^8) Mice received VEGF Trap protein (aflibercept) subcutaneously two times per week at 25 mg/kg. For control groups, mice were treated with humanized Fc (Regeneron). DC101 (a rat IgG1 monoclonal antibody targeting mouse VEGFR2)[21] was produced by Antibody Solution from conditioned media of the cognate hybridoma ATCC HB-11534. SCID mice received thrice-weekly subcutaneous injections of DC101 or control rat IgG (Sigma) at 40 mg/kg for 2 weeks. The anti-VEGF-A monoclonal antibody (mAb) B20.4.1.1[20], or control anti-ragweed mAb (Genentech) were administered to C57Bl/6 mice at 5 mg/kg, 3x/week i. p. All animals studies were performed in accordance with the National Institutes of Health guidelines for use and care of live animals and were approved by the Stanford University Institutional Animal Care and Use Committee A3213-01.

Adenoviruses

The construction of Ad-sFlt1 (encoding N-terminal hemagglutinin-tagged murine soluble VEGFR1 containing the first three Ig domains), Ad Flk1-Fc (encoding a full-length murine soluble VEGFR2 ectodomain fused to mouse IgG2α Fc) and Ad Fc (encoding IgG2α Fc alone) have been previously described[16,42]. Human *Hif2αPN* was generated by site-directed

mutagenesis replacing Pro531 and Asn847 by alanines. The human *Hif1α* allele lacking the inhibitory oxygen-dependent degradation domain (*Hif1α ODD*) was a kind gift of Cecile Chartier; similar methods were used to generate human *Hif2α ODD*. To generate adenoviruses expressing various shRNAs, an adenoviral shRNA shuttle vector was generated in which a CMV promoter drives a GFP/3' UTR miR-30 expression cassette in an Ad strain 5 backbone. miR-30-flanked shRNA sequences against mouse *Hif2α*, *Irs2*, *Dec1* and *Dec2* were obtained from Open Biosystems and cloned into the miR-30 expression cassette via XhoI/EcoRI restriction sites. Sequence information available upon request. The human nSrebp-1c adenovirus for in vitro primary hepatocyte infection was from Eton Bioscience, Inc. The human nSrebp-1c adenovirus used for in vivo mouse experiments has been described[27]. All adenoviral inserts were cloned into the E1 region of E1⁻E3⁻ Ad strain 5 by homologous recombination. Adenoviruses were produced in 293 cells and purified by double CsCl gradient purification as described[16].

Glucose Tolerance Test

Glucose tolerance tests were performed by intraperitoneal injection of glucose (2 g kg^{-1} for non-diabetic mice and 0.5 g kg^{-1} for diabetic *db/db* mice) after a 16 h overnight fast. Tail whole blood samples were taken before injection (time 0) and at 15, 30, 60, and 120 min post-injection.

Insulin Tolerance Test

Insulin tolerance tests were performed by intraperitoneal injection of insulin (Eli Lilly) (0.75 U/kg for non-diabetic mice and 1.5 U/kg for diabetic *db/db* mice) after a 5 hour fast. Whole blood samples were collected from the tail before insulin injection (time 0) and at 15, 30, 60, and 120 minutes post-injection. Glucose levels were normalized to fasted glucose levels at time 0, and AUC was calculated in GraphPad Prism using a baseline of y=1.

Hyperinsulinemic euglycemia clamp study

Studies were performed by the Mouse Metabolic Pathophysiology Core (MMPC) at Vanderbilt University as previously described[43] Insulin clamps were performed on 5-h fasted mice. [3-^{3}H]glucose was primed (0.8 μCi) and continuously infused for a 120-min equilibration period (0.04 μCi/min) and a 2-h clamp period (0.08 μCi/min). Baseline blood or plasma parameters were determined in blood samples collected at −10 and −5 min. At t = 0, insulin infusion (2.0 mU·kg^{-1}·min^{-1}) was started and continued for 155 min. Blood glucose was clamped using a variable rate of glucose infusion (GIR). Mice received heparinized saline-washed erythrocytes from donors at 4.5 μL/min to prevent a fall of hematocrit. Insulin clamps were validated by assessment of blood glucose over time. Blood glucose was monitored every 10 min, and the GIR was adjusted as needed. Blood was taken at 80–120 min for the determination of [3-^{3}H]glucose. Clamp insulin was determined at t = 120 and 155 min. At 120 min, 13 μCi of 2[^{14}C]deoxyglucose ([^{14}C]2DG) was administered as an intravenous bolus. Blood was taken at 2–35 min for the determination of [^{14}C]2DG. After the last sample, mice were anesthetized and tissues were collected. Plasma insulin was determined by the Vanderbilt Hormone Assay and Analytical Services Core. Radioactivity of [3-^{3}H]glucose, [^{14}C]2DG, and [^{14}C]2DG-6-phosphate were determined by liquid

scintillation counting. Glucose appearance (R_a) and disappearance (R_d) rates were determined using non-steady-state equations[44]. Endogenous glucose production (endoR_a) was determined by subtracting the GIR from total R_a. The glucose metabolic index (R_g) was calculated as previously described[45].

FACS-based hypoxia detection

C57BL/6 mice were injected intravenously with Fc, Flt1, and Flk1 adenoviruses as described above. At day 14, mice were injected intraperitoneal with pimonidazole hydrochloride 100 mg/kg (Hypoxyprobe, Inc., Burlington MA), and liver was harvested after 2 hours and disassociated into a single cell suspension using Collagenase IV (Sigma), permeabilized with TritonX, and incubated for one hour with FITC-conjugated anti-hypoxyprobe antibody (Hypoxyprobe, Inc., Burlington MA). Cells were analyzed on a BD LSR II Flow Cytometer (Becton Dickinson) using FlowJo software.

Quantitation of microvessel density

Vessel area density percentage of CD31 immunhistochemical and immunofluorescence sections (n 5 fields) were analyzed by pixel intensity measurements in ImageJ.

RNA isolation and real-time PCR

Total RNA was isolated using Trizol (Invitrogen). RNA samples were reversed transcribed into cDNA using a reverse transcription kit (Invitrogen). Individual gene expression was quantified by SYBR green real-time PCR (Biorad) and normalized to β-actin. Primer sequences for real-time PCRs are available upon request.

ELISA

Serum insulin was measured by enzyme-linked immunosorbent assay (ALPCO). Serum glucagon was measured by mouse glucagon ELISA (ALPCO).

Protein Immunoblot

The antibodies used were β-actin and GAPDH (Abcam); IRS1 and IRS2 (Millipore); AKT, p-AKT, GSK3β, p-GSK3β, FOXO1, and p-FOXO1 (Cell Signaling); anti-HIF2α (Santa-Cruz); anti-HIF1α (Bethyl). The following antibodies were from Cell Signaling: p-ACC1, ACC1, AMPKα, p-AMPKα, AMPKβ, p-AMPKβ. Liver lysates were prepared in RIPA buffer. Liver nuclear extracts were prepared using previously described nuclear extraction protocols[9]. Quantifications were performed by chemoluminescence and densitometric scanning of the films under linear exposure conditions. Phosphorylated-AKT was normalized to total AKT, phosphorylated-GSK3β was normalized to total GSK3β and IRS2 was normalized to actin loading control.

Isolation and culture of primary mouse hepatocytes

Primary hepatocytes were isolated from 10–12 week-old C57Bl/6 mice using a collagenase perfusion method from UCSF Liver Center (SFGH, San Francisco, CA). Isolated hepatocytes were resuspended in William's E media and plated on collagen I-coated plates in serum-free media. For hypoxia chamber experiments, cells were incubated at the specific O_2

concentration for 24 h followed by RNA extraction and gene expression analysis. For *in vitro* insulin stimulation assay, freshly harvested mouse primary hepatocytes were cultured in serum overnight. Adenoviruses were added to serum-free media 12 hours after plating for 24 hours at a multiplicity of infection (M.O.I) of 10 (Ad Fc, Ad HIF2αPN and Ad HIF1 ODD) or MOI of 20 (Ad shRNA IRS2 and Ad shRNA luciferase). Following adenoviral infection, cells were stimulated with 100 nM bovine pancreas insulin (Sigma) for 10 minutes followed by protein extraction and western blot analysis. For *in vitro Irs2* and *Srebp-1c* expression analysis, primary hepatocytes were infected with adenovirus 12 hours after plating for 24 hours at a M.O.I of 10 in serum-free media. After 24 hours, cells were stimulated with 10 nM insulin for 6 hours. RNA was extracted and qRT-PCR was performed as described above.

Lectin perfusion

Adult C57Bl/6 mice received single i.v. injection of Ad Fc, Ad sFlt1 or Ad VEGF Trap/ aflibercept[17] (encoding the aflibercept coding sequence) at 10^9 pfu each. Ad day 22, mice were anesthetized with Avertin and 100 μl of biotinylated L. esculentum lectin (1 mg/ml in 0.9% NaCl; Vector Laboratories) was injected by tail vein, allowed to circulate for 2 minutes and then the mouse was perfused with 1% PFA via the left ventricle. Paraffin sections of liver were developed with streptavidin-HRP and photographed at 20x magnification.

Transfections

Human IRS2 promoter-luciferase constructs containing wild-type sequence (wt) or mutations of the distal (−900mut) or proximal (−123mut) HREs were generated by site-directed mutagenesis and transfected into mouse H2 hepatocytes with internal Renilla luciferase control in the presence of Ad GFP, Ad Hif2α ODD or Ad Hif1α ODD.

Microarray analysis

For comparison of gene expression, 8–10 week-old female SCID C17 mice were injected with VEGF Trap (n = 5) or hFc (n = 4) at 25 mg/kg twice weekly for 9 weeks. RNA from liver was extracted as described above and 30 μg of total RNA was used to generate cDNA. Hybridization of sample cDNA to Mouse Exonic Evidence Based Oligonucleotide (MEEBO) arrays was performed by the Stanford Functional Genomics Facility (SFGF). Statistical analysis of gene expression was performed using Significance Analysis of Microarrays software (SAM) and heat-map representation was generated through TreeView.

Statistical analysis

All bars show mean ± s.e.m. Significance was calculated using a student's *t*-test or one-way ANOVA with Newman-Keuls post-test for comparison of groups greater than 2. * = $P <$ 0.05.

Supplementary Material

Refer to Web version on PubMed Central for supplementary material.

Acknowledgements

References

1. Leavens KF, Birnbaum MJ. Insulin signaling to hepatic lipid metabolism in health and disease. Crit Rev Biochem Mol Biol. 2011; 46:200–215. [PubMed: 21599535]

2. Taniguchi CM, Emanuelli B, Kahn CR. Critical nodes in signalling pathways: insights into insulin action. Nat Rev Mol Cell Biol. 2006; 7:85–96. [PubMed: 16493415]

3. Jungermann K. Zonation of metabolism and gene expression in liver. Histochem Cell Biol. 1995; 103:81–91. [PubMed: 7634156]

4. Kubota N, et al. Dynamic functional relay between insulin receptor substrate 1 and 2 in hepatic insulin signaling during fasting and feeding. Cell Metab. 2008; 8:49–64. [PubMed: 18590692]

5. Dong X, et al. Irs1 and Irs2 signaling is essential for hepatic glucose homeostasis and systemic growth. The Journal of clinical investigation. 2006; 116:101–114. [PubMed: 16374520]

6. Dong XC, et al. Inactivation of hepatic Foxo1 by insulin signaling is required for adaptive nutrient homeostasis and endocrine growth regulation. Cell Metab. 2008; 8:65–76. [PubMed: 18590693]

7. Zhong L, et al. The histone deacetylase Sirt6 regulates glucose homeostasis via Hif1alpha. Cell. 2010; 140:280–293. [PubMed: 20141841]

8. Hu CJ, et al. Differential regulation of the transcriptional activities of hypoxia-inducible factor 1 alpha (HIF-1alpha) and HIF-2alpha in stem cells. Mol Cell Biol. 2006; 26:3514–3526. [PubMed: 16611993]

9. Rankin EB, et al. Hypoxia-inducible factor-2 (HIF-2) regulates hepatic erythropoietin in vivo. J Clin Invest. 2007; 117:1068–1077. [PubMed: 17404621]

10. Kaelin WG Jr. Ratcliffe PJ. Oxygen sensing by metazoans: the central role of the HIF hydroxylase pathway. Mol Cell. 2008; 30:393–402. [PubMed: 18498744]

11. Ferrara N, Gerber HP, LeCouter J. The biology of VEGF and its receptors. Nature medicine. 2003; 9:669–676.

12. Alitalo K, Carmeliet P. Molecular mechanisms of lymphangiogenesis in health and disease. Cancer Cell. 2002; 1:219–227. [PubMed: 12086857]

13. Kamba T, et al. VEGF-dependent plasticity of fenestrated capillaries in the normal adult microvasculature. Am J Physiol Heart Circ Physiol. 2006; 290:H560–576. [PubMed: 16172168]

14. Billemont B, et al. Blood glucose levels in patients with metastatic renal cell carcinoma treated with sunitinib. British journal of cancer. 2008; 99:1380–1382. [PubMed: 18841151]

15. Hagberg CE, et al. Targeting VEGF-B as a novel treatment for insulin resistance and type 2 diabetes. Nature. 2012; 490:426–430. [PubMed: 23023133]

16. Kuo CJ, et al. Comparative evaluation of the antitumor activity of antiangiogenic proteins delivered by gene transfer. Proc Natl Acad Sci USA. 2001; 98:4605–4610. [PubMed: 11274374]

17. Tam BY, et al. VEGF modulates erythropoiesis through regulation of adult hepatic erythropoietin synthesis. Nature medicine. 2006; 12:793–800.

18. Papadopoulos N, et al. Binding and neutralization of vascular endothelial growth factor (VEGF) and related ligands by VEGF Trap, ranibizumab and bevacizumab. Angiogenesis. 2012; 15:171–185. [PubMed: 22302382]

19. Holash J, et al. VEGF-Trap: a VEGF blocker with potent antitumor effects. Proc Natl Acad Sci USA. 2002; 99:11393–11398. [PubMed: 12177445]

20. Liang WC, et al. Cross-species vascular endothelial growth factor (VEGF)-blocking antibodies completely inhibit the growth of human tumor xenografts and measure the contribution of stromal VEGF. J Biol Chem. 2006; 281:951–961. [PubMed: 16278208]

21. Prewett M, et al. Antivascular endothelial growth factor receptor (fetal liver kinase 1) monoclonal antibody inhibits tumor angiogenesis and growth of several mouse and human tumors. Cancer Res. 1999; 59:5209–5218. [PubMed: 10537299]

22. Fan X, et al. VEGF blockade inhibits angiogenesis and reepithelialization of endometrium. Faseb J. 2008; 22:3571–3580. [PubMed: 18606863]

23. Mancuso MR, et al. Rapid vascular regrowth in tumors after reversal of VEGF inhibition. J Clin Invest. 2006; 116:2610–2621. [PubMed: 17016557]

24. Canettieri G, et al. Dual role of the coactivator TORC2 in modulating hepatic glucose output and insulin signaling. Cell metabolism. 2005; 2:331–338. [PubMed: 16271533]

25. Ide T, et al. SREBPs suppress IRS-2-mediated insulin signalling in the liver. Nature cell biology. 2004; 6:351–357. [PubMed: 15048126]

26. Shimomura I, et al. Decreased IRS-2 and increased SREBP-1c lead to mixed insulin resistance and sensitivity in livers of lipodystrophic and ob/ob mice. Mol Cell. 2000; 6:77–86. [PubMed: 10949029]

27. Lecomte V, et al. A new role for sterol regulatory element binding protein 1 transcription factors in the regulation of muscle mass and muscle cell differentiation. Mol Cell Biol. 2010; 30:1182–1198. [PubMed: 20028734]

28. Yeo EJ, Cho YS, Kim MS, Park JW. Contribution of HIF-1alpha or HIF-2alpha to erythropoietin expression: in vivo evidence based on chromatin immunoprecipitation. Ann Hematol. 2008; 87:11–17. [PubMed: 17712557]

29. Covello KL, et al. HIF-2alpha regulates Oct-4: effects of hypoxia on stem cell function, embryonic development, and tumor growth. Genes Dev. 2006; 20:557–570. [PubMed: 16510872]

30. Mastrogiannaki M, et al. HIF-2alpha, but not HIF-1alpha, promotes iron absorption in mice. J Clin Invest. 2009; 119:1159–1166. [PubMed: 19352007]

31. Shah YM, Matsubara T, Ito S, Yim SH, Gonzalez FJ. Intestinal hypoxia-inducible transcription factors are essential for iron absorption following iron deficiency. Cell Metab. 2009; 9:152–164. [PubMed: 19147412]

32. Rankin EB, et al. Hypoxia-inducible factor 2 regulates hepatic lipid metabolism. Mol Cell Biol. 2009; 29:4527–4538. [PubMed: 19528226]

33. Wang XL, et al. Ablation of ARNT/HIF1beta in liver alters gluconeogenesis, lipogenic gene expression, and serum ketones. Cell Metab. 2009; 9:428–439. [PubMed: 19416713]

34. Scully MS, et al. A novel EPO receptor agonist improves glucose tolerance via glucose uptake in skeletal muscle in a mouse model of diabetes. Exp Diabetes Res. 2011; 2011:910159. [PubMed: 21754921]

35. Meng R, Zhu D, Bi Y, Yang D, Wang Y. Erythropoietin inhibits gluconeogenesis and inflammation in the liver and improves glucose intolerance in high-fat diet-fed mice. PLoS One. 2013; 8:e53557. [PubMed: 23326455]

36. Mardilovich K, Shaw LM. Hypoxia regulates insulin receptor substrate-2 expression to promote breast carcinoma cell survival and invasion. Cancer Res. 2009; 69:8894–8901. [PubMed: 19920186]

37. Qu A, et al. Hypoxia-inducible transcription factor 2alpha promotes steatohepatitis through augmenting lipid accumulation, inflammation, and fibrosis. Hepatology. 2011; 54:472–483. [PubMed: 21538443]

38. Bracken CP, et al. Cell-specific regulation of hypoxia-inducible factor (HIF)-1alpha and HIF-2alpha stabilization and transactivation in a graded oxygen environment. The Journal of biological chemistry. 2006; 281:22575–22585. [PubMed: 16760477]

39. Ho VW, et al. A low carbohydrate, high protein diet slows tumor growth and prevents cancer initiation. Cancer Res. 2011; 71:4484–4493. [PubMed: 21673053]

40. Gruber M, et al. Acute postnatal ablation of Hif-2alpha results in anemia. Proc Natl Acad Sci USA. 2007; 104:2301–2306. [PubMed: 17284606]

41. Postic C, et al. Dual roles for glucokinase in glucose homeostasis as determined by liver and pancreatic beta cell-specific gene knock-outs using Cre recombinase. J Biol Chem. 1999; 274:305–315. [PubMed: 9867845]

42. Jacobi J, et al. Discordant effects of a soluble VEGF receptor on wound healing and angiogenesis. Gene Ther. 2004; 11:302–309. [PubMed: 14737090]

43. Ayala JE, et al. Hyperinsulinemic-euglycemic clamps in conscious, unrestrained mice. J Vis Exp. 2011

44. Steele R, Wall JS, De Bodo RC, Altszuler N. Measurement of size and turnover rate of body glucose pool by the isotope dilution method. Am J Physiol. 1956; 187:15–24. [PubMed: 13362583]

45. Mulligan KX, Morris RT, Otero YF, Wasserman DH, McGuinness OP. Disassociation of muscle insulin signaling and insulin-stimulated glucose uptake during endotoxemia. PLoS One. 2012; 7:e30160. [PubMed: 22276152]
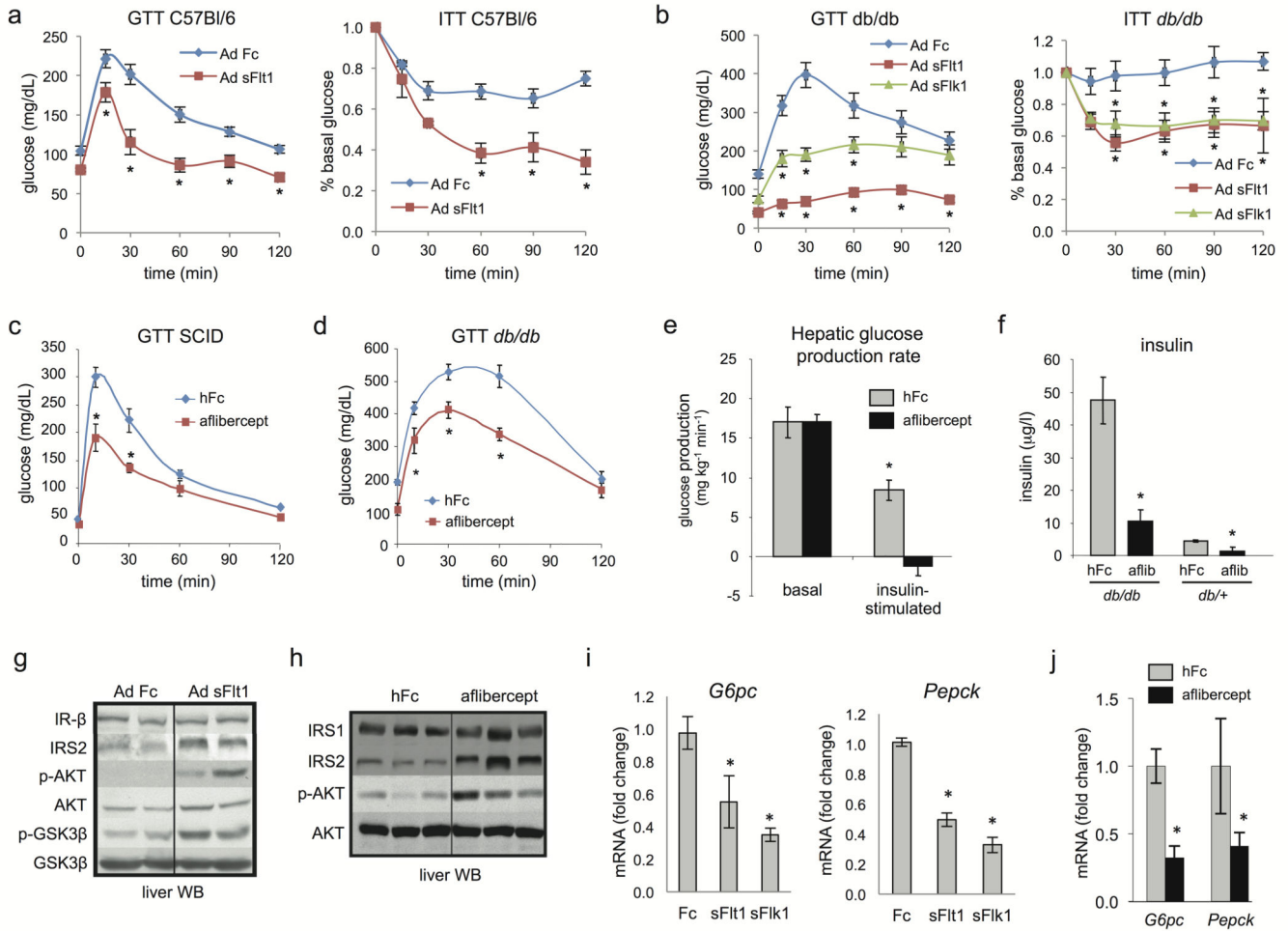
Figure 1. VEGF inhibition improves hepatic insulin action

a–d. Glucose tolerance tests (GTT) and insulin tolerance tests (ITT) in adult C57Bl/6J (a) or *db/db* mice (b) treated with a single i.v. injection of Ad sFlt1/sVEGFR1, Ad sFlk1/sVEGFR2 or Ad Fc (n=8 each, 10^9 pfu) after 15 days. The initial average blood glucose levels for ITT in a. were Fc=129, sFlt1=72.8 and in b. were Fc=162, sFlt1=55.4, sFlk1=109, all mg/dL. **c,d.** GTT of adult SCID mice (n=5) or db/db mice (n=5) treated with aflibercept or hFc after 15 days. **e.** Hyperinsulinemic euglycemic clamp analysis of aflibercept- and hFc-treated *db/db* mice after 2 weeks. **f.** ELISA determination of fasting plasma insulin concentration from mice as in d. **g,h.** Insulin signaling pathway determination in fasted liver extracts after 14 days. **i,j.** Analysis of *G6pc* and *Pepck* mRNA by qRT-PCR from liver from Ad Fc, Ad sFlt1 and Ad sFlk1-injected mice (n=5, ad lib, day 14) (i) or adult SCID mice treated with aflibercept, (n=5, fasted, day 14) (j). Values are expressed as mean ± s.e.m. * = P<0.05.

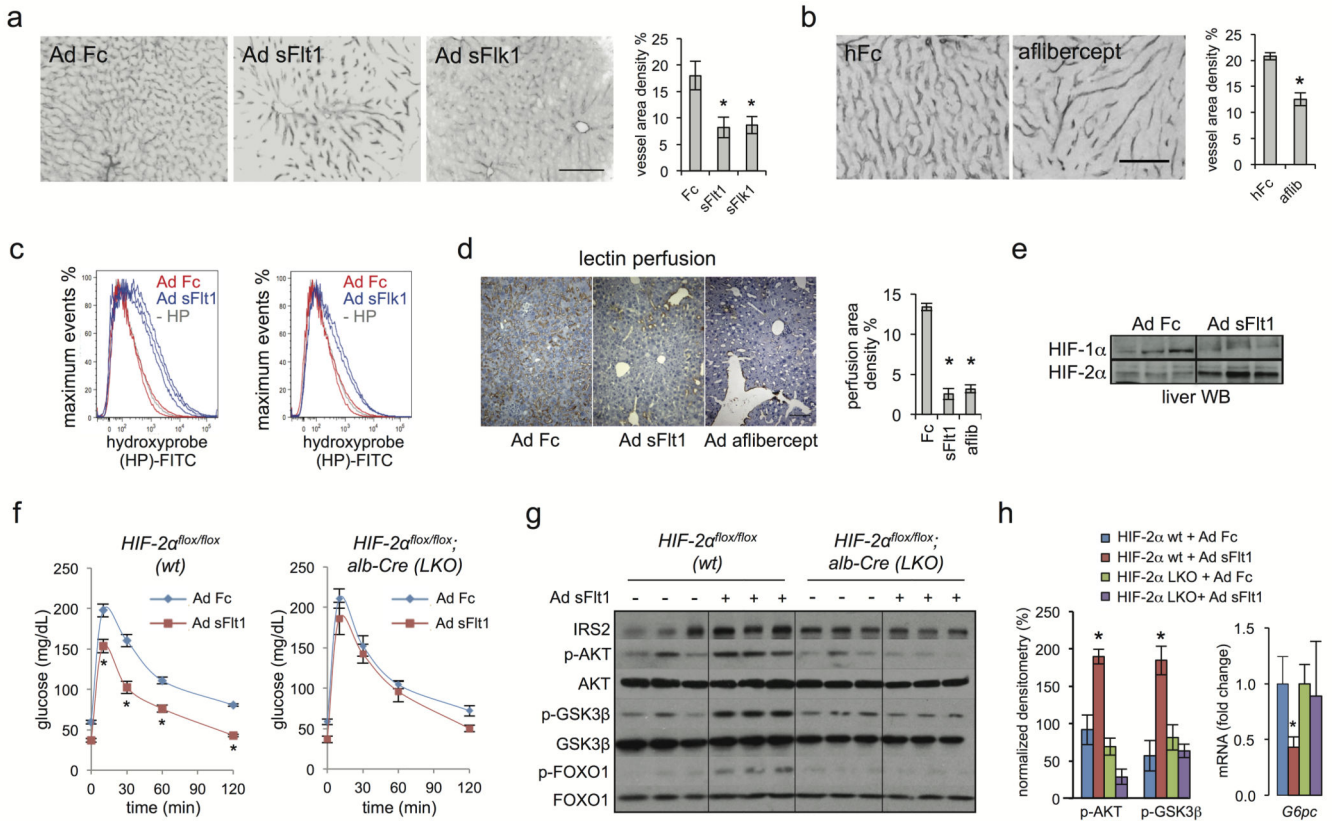**Figure 2. VEGF inhibition induces hepatic vascular regression, liver hypoxia and HIF-2α stabilization to augment hepatic insulin signaling**

a, b. Liver CD31 immunofluorescence and vessel area density percentage following Ad Fc, Ad sFlt1, Ad sFlk1, or aflibercept treatment after 14 days. Scale bar = 100 μm. **c.** FACS determination of hypoxia in mouse hepatocytes 14 days after Ad sFlt1-, Ad Flk1- (blue curves) or control Ad Fc- (red curves) treatment. Hypoxyprobe injection in mice was followed by anti-hydroxyprobe FITC-conjugated secondary antibody in disaggregated hepatocytes. The gray curve indicates a control liver without hypoxyprobe injection. **d.** Streptavidin-HRP staining of biotinylated *L. esculentum* lectin liver perfusion 22 days after Ad Fc, Ad sFlt1 and aflibercept treatment. Quantification of perfusion area density percentage is shown (n=3). **e.** HIF-2α and HIF-1α liver nuclear protein levels after 5 days Ad Fc and Ad sFlt1 treatment. **f.** GTT in 8–10 week old WT (Hif2α[flox/flox]) or HIF2LKO (Hif2α**flox/flox**; albumin-Cre) mice (n=6) 14 days after i.v. injection with Ad sFlt1 or Ad Fc. **g.** Liver Western blot from mice treated as in f. after 16 h fast. **h.** Densitometric quantitation of g. and *G6pc* liver qRT-PCR from f. Values are mean ± s.e.m. * = P<0.05.
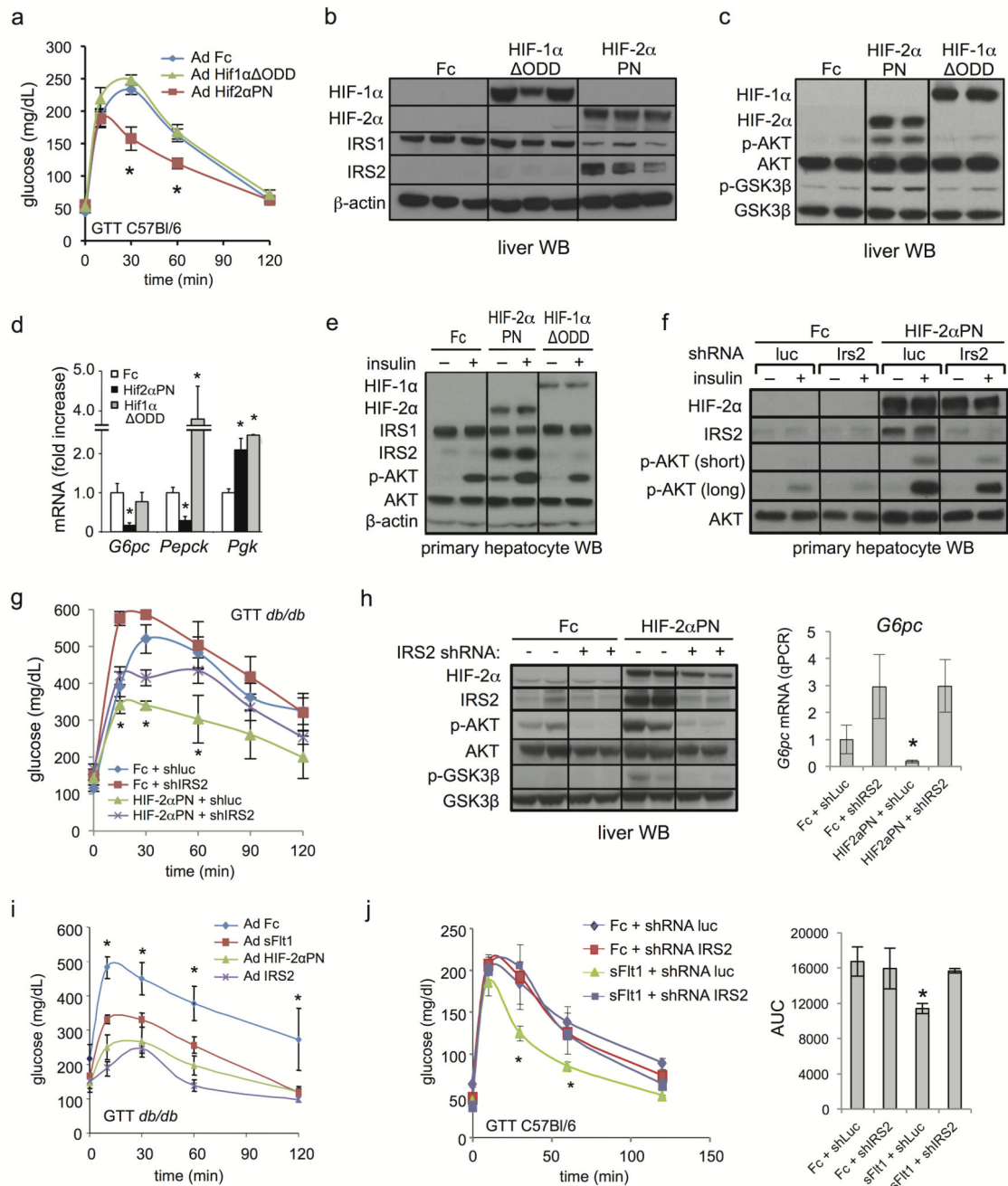
Figure 3. Activation of hepatic HIF-2α but not HIF-1α signaling is sufficient to improve liver insulin action

a. GTT of C57Bl/6 mice 3d after single i.v. injection of Ad Fc, Ad Hif1α ODD or Ad Hif2αPN. **b, c.** Liver extracts from animals in a. were analyzed by Western blot for IRS proteins (b) or for insulin signaling intermediates (c), 5d, ad lib. **d**. qPCR analysis of liver gluconeogenic gene expression, 5d, fasted. **e.** Western blot of hepatocytes 24 hours after Ad Fc, Ad Hif1α ODD or Ad Hif2αPN infection, with or without 100 nM insulin stimulation. **f.** Western blot of primary mouse hepatocytes infected with Ad Fc or Ad Hif2αPN +/− Ad

shRNA luc or Ad shRNA Irs2 for 24h, with and without 100 nM insulin stimulation. Short and long exposures for p-AKT are shown. **g.** GTT from *db/db* mice (n=8/group) 4 days after Ad Hif2αPN or Ad Fc treatment ± either Ad shRNA luciferase (shLuc) or Ad shRNA Irs2 (shIRS2). **h.** Western blot and qRT-PCR analysis of *G6pc* mRNA from liver of animals in g., ad lib. **i.** GTT from 8–10 week *db/db* mice treated with Ad Fc, Ad sFlt1, Ad Hif2αPN or Ad Irs2 after 5 days. **j.** GTT and AUC from C57Bl/6 mice at 5 days after injection with Ad Fc or Ad sFlt1 ± Ad shRNA luc or Ad shRNA Irs2 (n=6). Values are mean ± s.e.m. * = P<0.05.
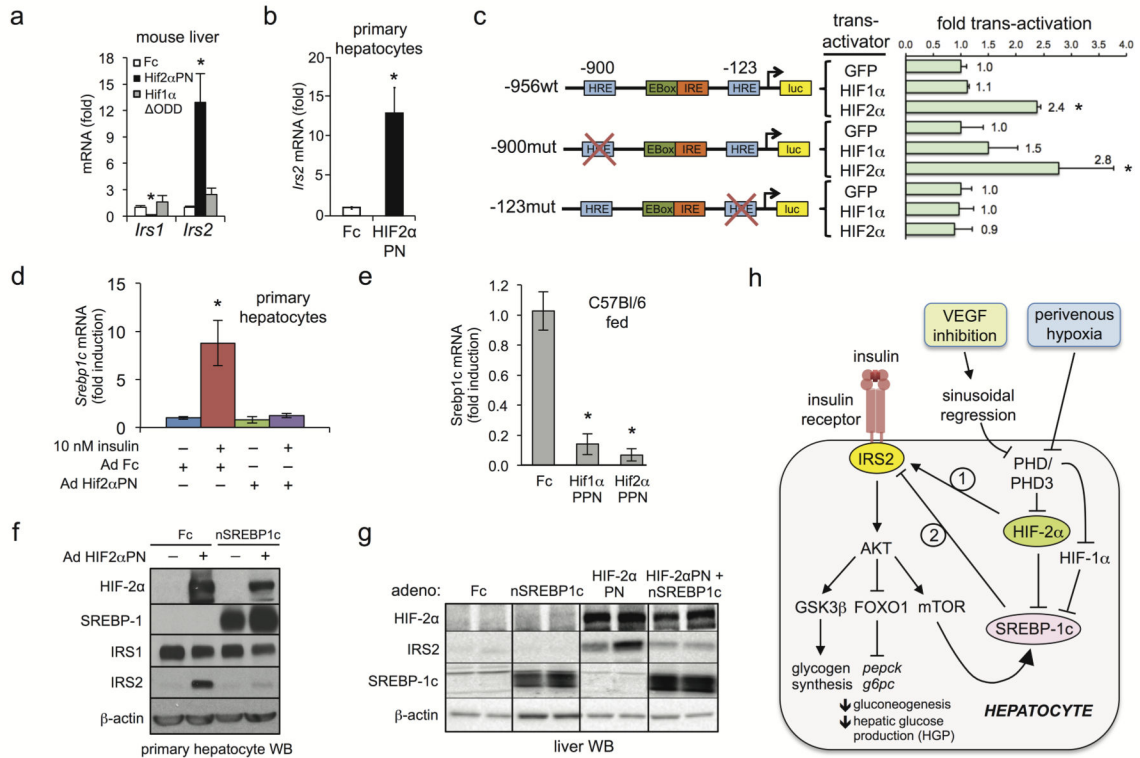
Figure 4. HIF-2α regulates IRS2 through Srebp1c-dependent and –independent mechanisms
a. qRT-PCR analysis of *Irs1* and *Irs2* in C57lBl/6 mouse liver 5 days after Ad Hif2αPN or Hif1α ODD treatment. **b.** qRT-PCR analysis of *IRS2* in primary hepatocytes 24h post-infection with the indicated adenoviruses. **c.** Luciferase reporter assay in mouse H2 hepatocytes with human *IRS2* promoter-luciferase constructs containing wild-type sequence (wt) or mutations of distal (−900mut) or proximal (−123mut) HREs with Ad GFP, Ad Hif2α ODD or Ad Hif1α ODD. **d.** *Srebp1c* qRT-PCR from primary hepatocytes infected with Ad Fc or Ad Hif2αPN ± insulin. **e.** Mouse liver *Srebp1c* qRT-PCR 5 days after Ad Fc, Ad Hif1α ODD or Ad Hif2αPN treatment. **f.** Western blot of primary hepatocytes infected with either Ad Fc or Ad Hif2αPN ± Ad nSrebp-1c. **g.** IRS2 and nSREPB1c liver Western blot after Ad Fc or Ad Hif2αPN treatment ± Ad nSrebp1c. **h.** Model. HIF-2α signaling positively regulates the insulin receptor signaling pathway in hepatocytes through induction of IRS2 expression. HIF-2α, but not HIF-1α regulates IRS2 expression directly by promoter trans-activation; both HIF-2α and HIF-1α suppress Srebp1c which can facilitate HIF2α transactivation of IRS2. Physiologic liver hypoxia and VEGF inhibition via vascular regression represent two stimuli capable of activating the HIF2α→IRS2 pathway, possibly mediated by PHD3 (see accompanying manuscript by Taniguchi et al.). Values are expressed as mean ± s.e.m. * = P<0.05.